In Proceedings of the 9th ESA Workshop on Advanced Space Technologies for Robotics and Automation
'ASTRA 2006' ESTEC, Noordwijk, The Netherlands, November 28-30, 2006

CASTING ROBOTIC END-EFFECTORS TO REACH FAR OBJECTS IN SPACE AND PLANETARY MISSIONS

Adriano Fagiolini[(1)], **Adriana Torelli**[(1)], **Antonio Bicchi**[(1)]

[(1)]***Interdepartmental Research Center "E. Piaggio"***
Faculty of Engineering - University of Pisa
Via Diotisalvi 2, 56126 Pisa, Italy
{***a.fagiolini, bicchi***}***@ing.unipi.it***

I. INTRODUCTION

In several space robotics applications as well as in planetary exploration missions, the possibility of reaching large workspace would afford great potential advantages. To operate on objects at distances several times larger than the physical dimensions of the robot, mobile platforms [1] equipped with articulated arms are practically the only available solution at the state of the art. However, wheeled or legged robotic locomotion depends heavily on the characteristics of the terrain, and is usually forced to trade velocity of execution for robustness to terrain asperities. As a matter of fact, e.g., Martian explorers Spirit and Opportunity have been traveling at max. 180 m/h speed, on an average mission length of 100 meters from the base station, thus limiting the number of samples returned per day. The alternative of building arms with either very long links [2] or many links [3], [4] seems to be applicable only in some very specific cases – for instance in the absence of gravity – and yet imposes the use of very wide mechanical structures despite the extension of their reachable spaces.

In this paper we present work aimed at developing a compact robotic device able to reach objects at far distance. The work is based on the idea of *casting manipulation*, a robotic technique that was proposed in [5], and that allows to deploy an end-effector at large distances from the robot's base by throwing (casting) it and controlling its ballistic flight using forces transmitted through a light tether connected to the end-effector itself. The tether cable of the robotic device can also be used to retrieve the end-effector, and to exert forces on the robot's environment. The operating phases of casting manipulation comprise a *startup phase*, a *steering phase*, and an *object-return phase*. During the startup phase, the robot is controlled so as to impart the end-effector sufficient mechanical energy to reach the target-object. When the first phase concludes, the end-effector is thrown and its trajectory is steered by means of forces transmitted through the tether cable in order to approach the moving object with suitable orientation and velocity (steering phase). Once the object has been caught, the tether cable is reeled up and the object is retrieved (object-return phase). Fig. 1 depicts possible application of casting manipulation during sample-return missions (left), and outlines the different operating phases of the technique (right).

Ability of simple casting manipulator prototypes to fetch faraway fixed objects, controlling the position and orientation of the gripper and even avoiding obstacles, has been demonstrated in [6]–[8]. More recent work has extended applicability of the technique to reach targets with uncertain position, or that are possibly moving [9], by using simplified yet accurate models that are suitable for realtime computation, and visual feedback of the moving targets. Starting from that result, we will describe two control schemes of the steering phase: the first approach is simpler and

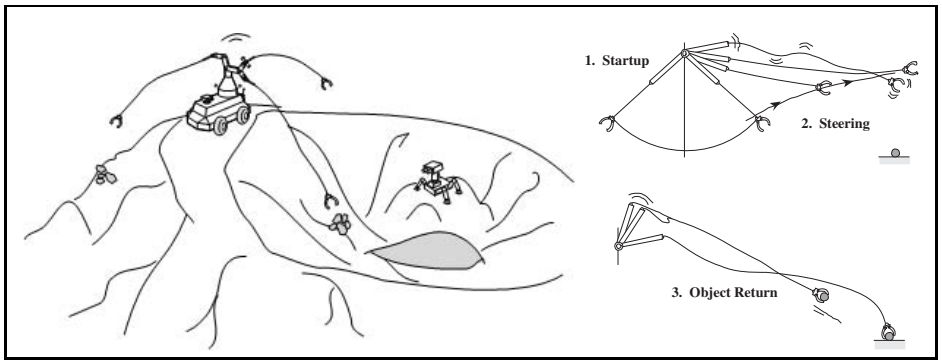

Fig. 1. A robotic end-effector connected to a manipulator through a light tether can be used to reach far away from the manipulator base. The end-effector can in fact be deployed at large distance by casting it and then controlling its ballistic flight. Possible application of casting manipulation in sample-return missions are depicted on the left, and different operating phases of the technique are outlined on the right. (Picture reprinted from [5])

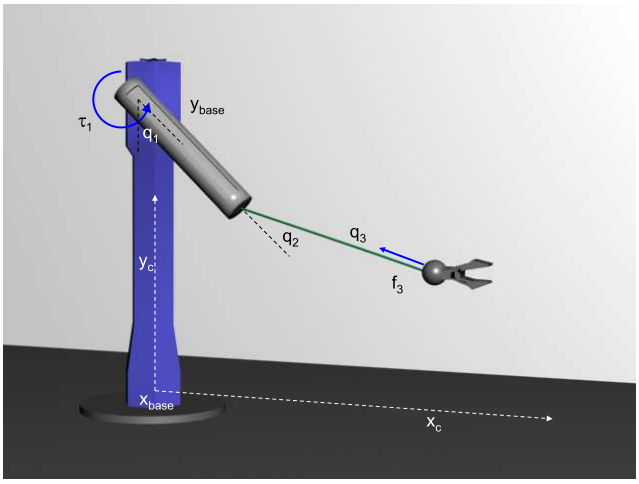

Fig. 2. Depiction of a planar casting manipulator consisting of a rigid link, a light tether, and a gripper.

exploits transmission of impulsive forces, whereas the second is computationally more expensive but is more general, and consists of steering the end-effector's flight by means of continuous force signals. Effectiveness of both steering methods has been demonstrated through experiments.

The extension of casting manipulation to the hypothesis of possibly moving objects has proved it viable for applications such as sample acquisition and return, rescue, etc. Nonetheless, only steering of the robotic end-effector along the throwing plane has been demonstrated so far. We also present work relating design and control of a novel compact manipulator allowing steering of the end-effector's trajectory in 3-dimensional space. Such a manipulator is composed of 3 tether cables that are connected to the end-effector, and to the edges of a triangular platform. The platform can rotate along an axis parallel to it and passing through its center of mass. Again, the rotation is used during the startup phase to impart the end-effector sufficient mechanical energy to reach the target, and visual feedback of objects is used to decide on the robot's throwing configuration.

Control of such "cable-driven" manipulators is challenging due to limitation in admissible control inputs, i.e. each robot actuator is able to generate only a pulling force with upper saturation (unilateral input constraints). In this context, we formulate and find solution of a time-optimal control problem – steering the end-effector in minimum-time – as generalization of the continuous control scheme applied to planar casting. Optimization concerns also the choice of the throwing angle with respect to the direction of the target. Effectiveness of the optimal solution has been checked through simulation.

The paper is organized as follows. Section II deals with modeling and control of a planar casting manipulator, and presents the two aforementioned control schemes allowing realtime planning of an end-effector's trajectory. Then, in Section III, we deal with design and time-optimal control of a 3-dimensional casting manipulator, and present some preliminary results of the new technique. In Section IV, we show effectiveness of the two proposed steering methods of planar casting by reporting experimental results. Finally, work achievement are summarized in closing Section V. For more information see http://www.piaggio.ccii.unipi.it/newrobotics/casting.html.

II. Planar Casting Manipulation

A. Modeling and Control of the Robot

To begin with, consider the simple manipulator depicted in Fig. 2 that can be used for planar casting. The robot consists of a rigid link L_1 with revolute joint q_1 actuated by torque τ_1, and a controlled reel for winding and unwinding a tether cable. Angle q_2 at which the tether departs from the rigid link is measured but not actuated. The variable length q_3 of the tether can be viewed as a third link with translational joint actuated by the reeling force f_3. The robot's end-effector is a gripper.

Modeling of the robot's dynamics during the startup and steering phases would need particular attention due to elasticity and flexibility of the tether cable. Notwithstanding, a simplified model can be found in the hypothesis that the tether is never loose, and elastic modes are never excited (cf. e.g. [10]–[12]). Under this hypothesis the tether can be approximated as rigid, and the robot's dynamics can be written in the classical form:

$$\mathbf{B}(\mathbf{q})\,\ddot{\mathbf{q}} + \mathbf{C}(\mathbf{q},\dot{\mathbf{q}})\,\dot{\mathbf{q}} + \mathbf{G}(\mathbf{q}) = \boldsymbol{\tau}\,, \tag{1}$$

where $\mathbf{B} \in \mathbb{R}^{\mathbf{3\times 3}}$, $\mathbf{C} \in \mathbb{R}^{\mathbf{3\times 3}}$, $\mathbf{G} \in \mathbb{R}^{\mathbf{3}}$, $\mathbf{q} = (q_1, q_2, q_3)^T$, and $\boldsymbol{\tau} = (\tau_1, 0, -f_3)^T$. It is worth noting that control input f_3, representing the pulling force transmitted through the tether to the end-effector, can not become negative: $f_3(t) \geq 0$.

To control the manipulator one has to deal with its underactuation, namely we have two controls τ_1 and f_3 but three joint variables q_1, q_2, and q_3. However, a control strategy of underactuated mechanisms is proposed in [13], basically suggesting to use available inputs to steer the dynamics of a subset of joints, and then to control such joints in order to indirectly excite the others. To this aim, we left-multiply (1) by inverse of inertia matrix $\mathbf{B}$, and thus obtain: $\ddot{\mathbf{q}} = \mathbf{B}^{-1}\ (\boldsymbol{\tau} - \mathbf{C}\,\dot{\mathbf{q}} - \mathbf{G})$. This vector equation can be expanded as

$$\begin{pmatrix} \ddot{q}_1 \\ \ddot{q}_2 \\ \ddot{q}_3 \end{pmatrix} = \begin{pmatrix} b_{11} & b_{12} & b_{13} \\ b_{21} & b_{22} & b_{23} \\ b_{31} & b_{32} & b_{33} \end{pmatrix}^{-1} \begin{pmatrix} \gamma_1 + \tau_1 \\ \gamma_2 \\ \gamma_3 - f_3 \end{pmatrix},$$

where γ_1, γ_2, and γ_3 are linear combinations of elements of matrix $\mathbf{C}$ with coefficients $\dot{q}_1$, $\dot{q}_2$, and $\dot{q}_3$, plus elements of vector $\mathbf{G}$. It can be shown that the manipulator's dynamics can partially be linearized by suitable choice of control inputs τ_1 and f_3, and the remaining zero-dynamics can be made asympotically stable. We will omit explicit calculation due to space limitation.

Under the same hypothesis of preventing tether slackness, also the end-effector's state can easily be related to the joint variables through direct and differential kinematics equations. In fact, the end-effector position (x_e, y_e) and orientation φ_e with respect to axis x are given by:

$$\begin{cases} x_e = x_{base} + a_1\, S_1 + q_3\, S_{12}\,, \\ y_e = y_{base} - a_1\, C_1 - q_3\, C_{12}\,, \\ \varphi_e = q_1 + q_2 + \frac{\pi}{2}\,, \end{cases} \tag{2}$$

where (x_{base}, y_{base}) is position of the robot's base[1]. Furthermore, linear and angular velocities of the end-effector are related to the joint variables velocities through the jacobian matrix:

$$\begin{pmatrix} \dot{x}_e \\ \dot{y}_e \\ \dot{\varphi}_e \end{pmatrix} = \begin{pmatrix} a_1\, C_1 + q_3\, C_{12} & q_3\, C_{12} & S_{12} \\ a_1\, S_1 + q_3\, S_{12} & q_3\, S_{12} & -C_{12} \\ 1 & 1 & 0 \end{pmatrix} \begin{pmatrix} \dot{q}_1 \\ \dot{q}_2 \\ \dot{q}_3 \end{pmatrix}. \tag{3}$$

B. Realtime Computation of End-effector's Trajectory

During the steering phase, the end-effector is controlled in order to reach the target-object at point (x_t, y_t) with suitable orientation φ_e, and velocities $(\dot{x}_e, \dot{y}_e, \dot{\varphi}_e)$. A control policy of a gripper ballistic flight was proposed in [6], [7], [14], consisting of transmition of a series of impulses through the tether cable. Effectiveness and accuracy of the method were shown through experiments when position of the target-object was fixed. However, the approach is inadequate when the object position is uncertain or the object itself is moving, since it is based on precise *a priori* knowledge of the position, and needs long computation times. In [9], applicability of planar casting manipulation has recently been extended to deal with this last case, by using simplified yet accurate models that are suitable for realtime computation, and visual feedback of the moving targets. Starting from that result, we will now describe two control schemes of the steering phase. Since we are not dealing with gripper orientation at present, we will replace the end-effector with a mass point m.

The first approach is simpler and exploits transmission of impulsive forces to steer the end-effector's flight and eventually control its landing position. Fig. 3 is a depiction of possible end-effector's trajectories under this impulse-based control scheme. The strategy can be summarized as follows. After initial target position is estimated, the end-effector is thrown at time t_0 and the tether starts unwinding. If no force is transmitted, i.e. $f_3(t) = 0$ for $t \geq t_0$, the end-effector moves along an arc of parabola, eventually landing on the point represented by $(x_{land-max}, 0)$ where

$$x_{land-max} = x_e(t_0) + \frac{\dot{x}_e(t_0)}{2\,g}\left(\dot{y}_e(t_0) + \sqrt{\dot{y}_e(t_0)^2 + 2\,g\,y_e(t_0)}\right),$$

g is the gravity acceleration, and the initial state $x_0 = (x_e(t_0), y_e(t_0), \dot{x}_e(t_0), \dot{y}_e(t_0))$ is evaluated from (2) and (3). Moreover, before throwing, a *braking time* is decided such that the tether length equals the distance between the "estimated" target position and the robot's base. At that time, control input f_3 is used to stop the tether unwinding and to fix its length, thus constraining the end-effector to move along the arc of circumference BC leading it over the desired target position. If the target-object comes nearer the robot's base or recedes from it, the pre-planned braking time is anticipated or delayed, accordingly.

[1]The following standard abbreviations are used: $C_i = \cos(q_i)$, $S_i = \sin(q_i)$, $C_{ij} = \cos(q_i + q_j)$ and $S_{ij} = \sin(q_i + q_j)$.

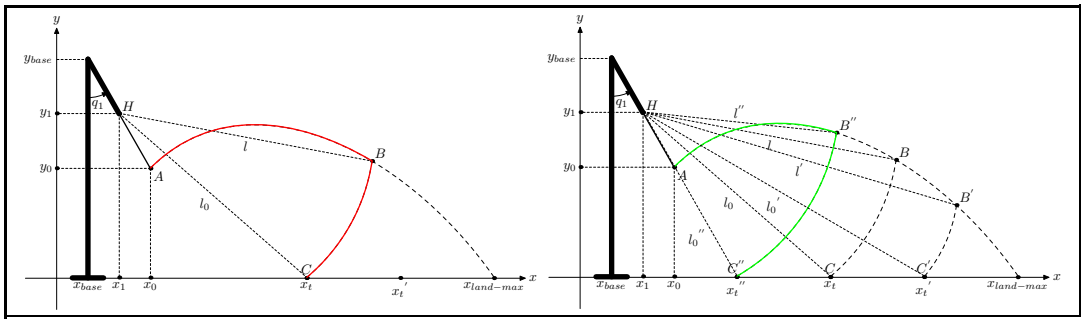

Fig. 3. Depiction of possible end-effector's trajectories under impulse-based control scheme of the steering phase.

The second approach is computationally more expensive but is more general, and consists of steering the end-effector's flight by means of continuous forces. From geometric consideration on Fig. 2, we can obtain the end-effector's dynamics:

$$\begin{cases} \ddot{x}_e = -\frac{1}{m}\,\sin\left[\tan^{-1}\left(\frac{x_e - x_{L_1}}{y_e - y_{L_1}}\right)\right]\,u\,, \\ \ddot{y}_e = -g - \frac{1}{m}\,\cos\left[\tan^{-1}\left(\frac{x_e - x_{L_1}}{y_e - y_{L_1}}\right)\right]\,u\,, \end{cases}$$

where (x_{L_1}, y_{L_1}) is the point where the tether departs from the rigid link, and u is the transmitted force. After some simplifications we can re-write the end-effector's dynamics as:

$$\begin{cases} \ddot{x}_e = -\frac{1}{m}\,\dfrac{\frac{x_e - x_{L_1}}{y_e - y_{L_1}}}{\sqrt{1+\left(\frac{x_e - x_{L_1}}{y_e - y_{L_1}}\right)^2}}\,u\,, \\ \ddot{y}_e = -g - \frac{1}{m}\,\dfrac{1}{\sqrt{1+\left(\frac{x_e - x_{L_1}}{y_e - y_{L_1}}\right)^2}}\,u\,. \end{cases}$$

Let $x = (x_e, y_e, \dot{x}_e, \dot{y}_e)$ be the end-effector state, x_0 be its initial value at the throwing time, and $x_f = (x_t, y_t)$ be the desired landing position. The end-effector's dynamics can easily be written in state form as $\dot{x}(t) = f(x(t), u(t))$. Let also u_{max} be the maximum force that can be transmitted through the cable. Then, the end-effector can be steered from state x_0 to x_f in unknown minimum time t_f, by finding a control function $\bar{u} : [t_0, t_f] \rightarrow [0, u_{max}]$ that solves the following dynamic programming problem:

$$\begin{cases} \bar{u}(t) = \arg\min_{u(t)} J\,, \\ J = \int_{t_0}^{t_f} 1\,d\tau\,, \\ \dot{x}(t) = f(x(t), u(t))\,, \\ x(t_0) = x_0\,, \\ x(t_f) = x_f\,, \\ -u(t) \leq 0\,, \\ u(t) \leq u_{max}\,. \end{cases} \tag{4}$$

III. 3-DIMENSIONAL CASTING MANIPULATION

In this section we introduce a new casting manipulator that is able to steer the end-effector's flight in 3D space, thus extending applicability of the technique to 3-dimensional casting. The robot is composed of 3 tether cables that are connected to the end-effector, and to the edges of a triangular platform (see Fig. 4). The platform can rotate along an axis parallel to it and passing through its center of mass. The rotation is used during the startup phase to impart the end-effector sufficient mechanical energy for reaching the target-object.

Modeling of the end-effector's dynamics during the steering phase can easily be done by doing some geometric consideration on the figure. Let (x_e, y_e, z_e) be the end-effector position, u_1, u_2, u_3 be the three actuation forces, α be the angle between the platform and the target direction, and α_0 be its value at the throwing time t_0. Then, the end-effector's dynamics is given by:

$$m \begin{pmatrix} \ddot{x}_e \\ \ddot{y}_e \\ \ddot{z}_e - g \end{pmatrix} = - \begin{pmatrix} \frac{x_e + b\,C_\alpha}{\gamma_1(x_e,y_e,z_e)} & \frac{x_e - b\,C_\alpha}{\gamma_2(x_e,y_e,z_e)} & \frac{x_e}{\gamma_3(x_e,y_e,z_e)} \\ \frac{y_e - b\,S_\alpha}{\gamma_1(x_e,y_e,z_e)} & \frac{y_e - b\,S_\alpha}{\gamma_2(x_e,y_e,z_e)} & \frac{y_e}{\gamma_3(x_e,y_e,z_e)} \\ \frac{z_e + b\frac{\sqrt{3}}{3}}{\gamma_1(x_e,y_e,z_e)} & \frac{z_e + b\frac{\sqrt{3}}{3}}{\gamma_2(x_e,y_e,z_e)} & \frac{z_e + b\frac{\sqrt{3}}{3}}{\gamma_3(x_e,y_e,z_e)} \end{pmatrix} \begin{pmatrix} u_1 \\ u_2 \\ u_3 \end{pmatrix}, \tag{5}$$

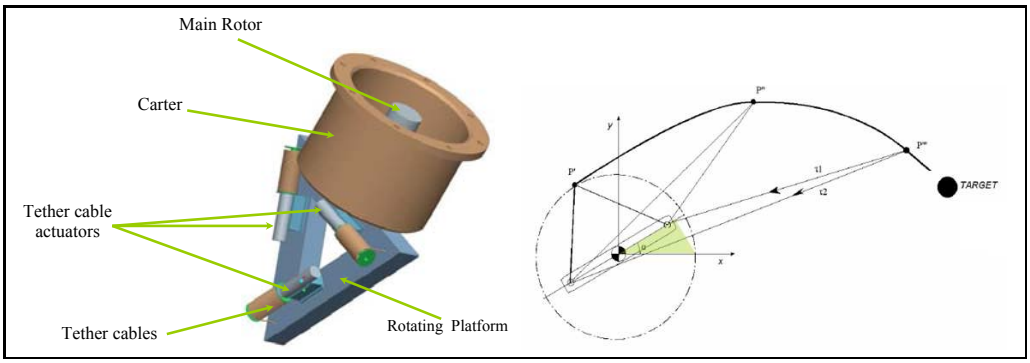

Fig. 4. Mechanical design (*left*) and top view projection (*right*) of a simple robot (DAVIDE) to be used for 3-dimensional casting manipulation.

where

$$\gamma_1(x_e, y_e, z_e) = \sqrt{(x_e + b\,C_\alpha)^2 + (y_e + b\,S_\alpha)^2 + \left(z_e + b\,\frac{\sqrt{3}}{3}\right)^2}\,,$$
$$\gamma_2(x_e, y_e, z_e) = \sqrt{(x_e - b\,C_\alpha)^2 + (y_e - b\,S_\alpha)^2 + \left(z_e + b\,\frac{\sqrt{3}}{3}\right)^2}\,,$$
$$\gamma_3(x_e, y_e, z_e) = \sqrt{x_e^2 + y_e^2 + \left(z_e + b\,\frac{2\sqrt{3}}{3}\right)^2}\,,$$

and b is the robot arm.

We are interested in generating time-optimal control functions for the considered "cable-driven" casting robot, minimizing the time needed to steer the end-effector toward a desired position in 3D-space. Challenge here is represented by input control bounds due to the fact that robot cables can exert only pulling forces (unilateral input bounds). The optimization also concerns choice of the throwing angle α_0 with respect to the target direction.

Let $x = (x_e, y_e, z_e, \dot{x}_e, \dot{y}_e, \dot{z}_e)$ be the end-effector's state, $u = (u_1, u_2, u_3)$ be the transmitted input vector force. Again, the system dynamics (5) can be written in state form $\dot{x}(t) = f(x(t), u(t), \alpha_0)$. Moreover, let ω_0 be the angular velocity of the rotating platform at the throwing time, then the initial state x_0 is obtained as:

$$x_0(\alpha_0, \omega_0) = (-r\,S_{\alpha_0}, r\,C_{\alpha_0}, 0, r\omega_0\,C_{\alpha_0}, r\,\omega_0\,S_{\alpha_0}, 0)\ .$$

Let $x_f = (x_t, y_t, z_t)$ be the target-object position, and u_{max} the maximum force that each actuator can provide. Then, the end-effector can be steered from state $x_0(\alpha_0)$ to x_f in unknown minimum time t_f, by finding the time-optimal control vector function $\bar{u} : [t_0, t_f] \rightarrow [0, u_{max}]$, and the optimal throwing angle $\bar{\alpha}_0 \in [0, 2\pi]$ that solve the following dynamic programming problem:

$$\begin{cases} [\bar{u}(t), \bar{\alpha}_0] = \arg\min_{[u(t),\alpha_0]} J\,, \\ J = \int_{t_0}^{t_f} 1\,d\tau\,, \\ \dot{x}(t) = f(x(t), u(t), \alpha_0)\,, \\ x(t_0) = x_0(\alpha_0)\,, \\ x(t_f) = x_f\,, \\ -u(t) \leq 0\,, \\ u(t) \leq u_{max}\,. \end{cases}$$

We have solved this dynamic optimization problem by using numerical tools, and obtained the results that are summarized in the following figures. Fig. 5 shows the optimal time $\bar{t}_f$ versus the relative throwing angle α_0, and reveals that the optimum value is $\bar{\alpha}_0 = 3\pi/4$ radiants. Fig. 6 shows the optimal time $\bar{t}_f$ at optimal throwing angle $\bar{\alpha}_0$ versus the target-object position: due to radial symmetry of the problem, optimal time depends only on the target distance. Furthermore, Fig. 7 shows the optimal control $\bar{u}(t)$ for a point-to-point motion, and corresponding state evolution in condition of no gravity ($g = 0\,m/s^2$), and with gravity ($g = 9.81\,m/s^2$).

IV. Experimental results of planar casting manipulation

We have developed a simple manipulator to test effectiveness of the two proposed control schemes of Section II for planar casting. The experimental setup is also composed of a control system, and a vision system providing a visual estimate of the current object position.

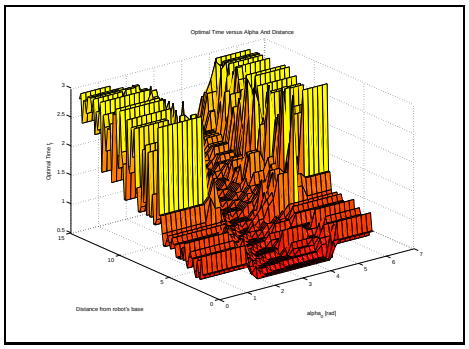

Fig. 5. Optimal time $\bar{t}_f$ versus throwing angle α_0 and target-object distance.

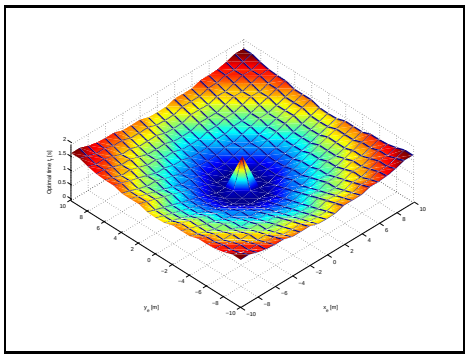

Fig. 6. Optimal time $\bar{t}_f$ at optimal throwing angle $\bar{\alpha}_0$ versus the target-object position.

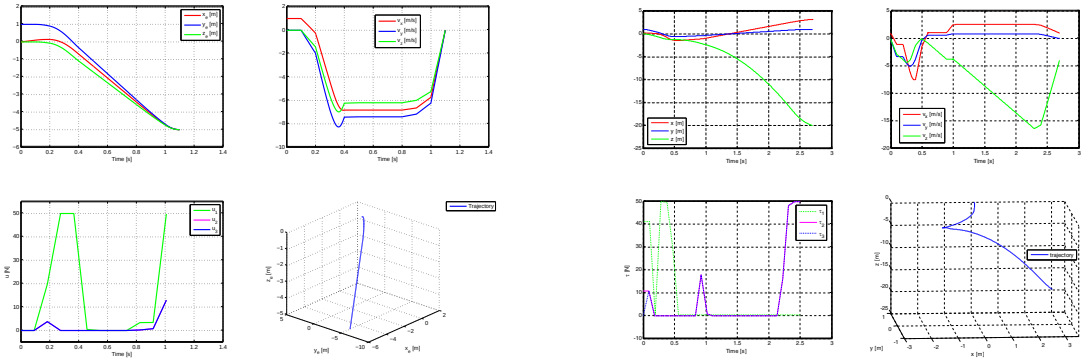

Fig. 7. Optimal control $\bar{u}(t)$ for a point-to-point motion, and corresponding state evolution in condition of no gravity ($g = 0\, m/s^2$) (*left*), and with gravity ($g = 9.81\, m/s^2$) (*right*).

A. The Robot

The manipulator realized in our lab is composed of a rigid link L_1 with revolute joint q_1 actuated by torque τ_1, a null-length link L_2 with another revolute joint q_2, and light tether cable L_3 with translational joint q_3 actuated by input force f_3. Since we are not dealing with orientation control at present, we have used a mass m as the robotic end-effector. Refer to Section II for the robot's and end-effector's dynamics, and to the table of Fig. 9 for geometrical and inertial parameters.

Optical encoders are used to read joint variable q_1, q_2, and q_3. In particular, an 81000 pulses per revolution (ppr) encoder is used for the first joint, and two 2048-ppr encoders for the other two joints. Two direct-driver motors have been used to generate input controls τ_1 and f_3. To control the tether unwinding control input f_3 is used as well as a braking mechanism. Fig. 8 shows the robot, and a detail of the brake.

B. Vision and Control Systems

Both vision and control systems have been implemented and hosted on a single Pentium© IV with clock frequency of 3.0 GHz. Still from a hardware point of view, a US Digital PCI4ES card has been used to read encoder data of the joint variables, and a National Instrument PCI6024E card has been used to control robot's inputs. The vision system takes advantage of a low-cost USB Logitech© Orbit camera with framerate of 16 fps. As far as concerning the software, the underlying platform was Microsoft Windows© XP, and all of the source code was written in C++ programming language. In particular, implementation of algorithms for calibration of the camera and object detection uses OpenCV© library functions. The control process was scheduled with cycletime of 0.5 msec. Fig. 10 shows an example of image processed by the vision system with detected items: target-object is highlighted in blue, and calibration markers are highlighted in red.

The vision system is easy to set up, hard to fail in tracking the target, and shows high precision once calibrated. Furthermore, the calibration procedure is very quick, and hence could be performed during the experiment if the camera is moved. The only demerit we observed is a long sampling time – around 62 msec is necessary to obtain a new data position – that restricts possible target velocities. However this fact is due to the low-cost camera, and can be solved by exploiting high-speed vision systems such as that in [15] that can achieve very short sampling time of 1 msec.

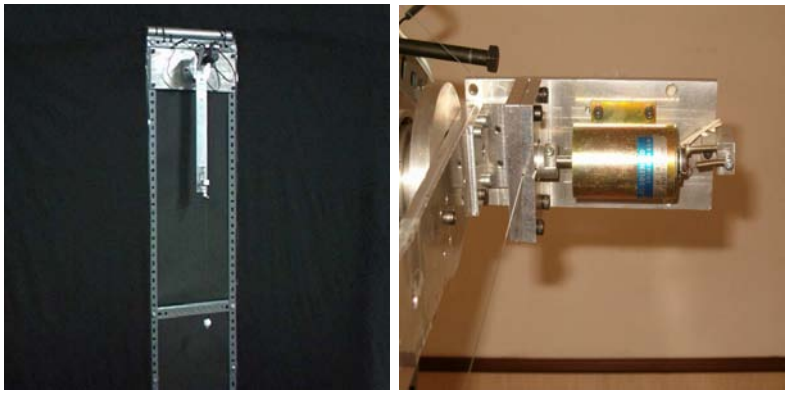

Fig. 8. The manipulator realized in our lab, and a detail of the brake.

Parameter	Value	Unit
x_{base}	0.000	m
y_{base}	1.695	m
a_1	0.342	m
m_1	1.1105	kg
I_1	0.0216	$kg\,m^2$
a_3	0.495	m
m_3	0.084	kg
I_3	1.3440E-005	$kg\,m^2$

Fig. 9. Inertial and geometrical parameters of the realized manipulator for planar casting.

Fig. 10. Example of image processed by the vision system with detected items: target-object is highlighted in blue, and calibration markers are highlighted in red.

C. Experiments

Experimental results of planar casting with moving objects are reported in Fig. 11: trajectories of the end-effector under impulse-based control scheme is traced out on the left, and trajectory under transmition of continuous time-optimal force is revealed on the right.

Effectiveness of the impulse-based control scheme of the steering phase has been checked through the following experiment. First a static object is set into the environment, and its position is estimated by the vision system. The end-effector is imparted sufficient mechanical energy to reach the target during the initial startup phase. After that the end-effector is casted, and the tether starts unwinding. When the tether length equals the distance between the target position and the point where the tether departs, the unwinding is stopped. As expected from theory, the end-effector's ballistic flight is composed of an arc of parabola and an arc of circumference corresponding to curves AB and BC of Fig. 3, respectively. Secondly, a similar experiment has been performed were the target-object moves after

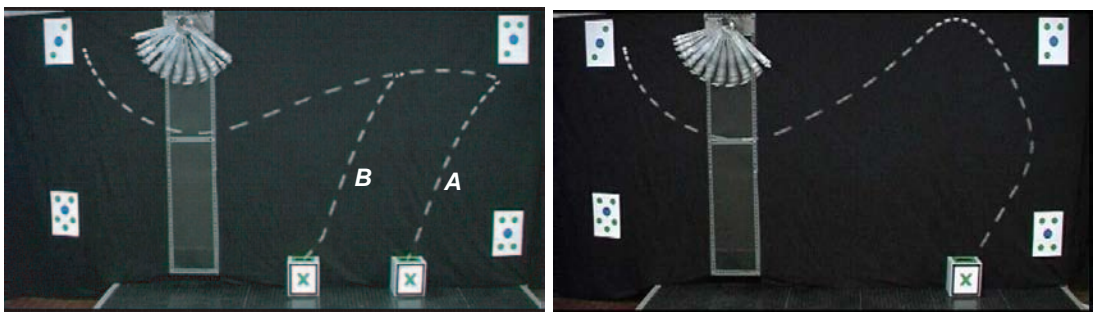

Fig. 11. Results of planar casting manipulation with moving target-objects. Trajectories of the end-effector under impulse-based control scheme is traced out on the left, and trajectory under transmition of continuous time-optimal force is revealed on the right.

the throwing coming nearer the robot's base. As expected from theory, the target is also reached by anticipating the pre-planned braking time. It is worth noting that the actual end-effector's trajectories after the braking can only be approximated by arc of circumferences, revealing that the hypothesis of tether unslackness becomes weaker after that moment. Nonetheless, the assumption has been necessary to achieve realtime computation requirements.

Effectiveness of the continuous time-optimal control scheme has also been tested where control inputs were computed by solving problem (4).

V. Conclusion

In this paper we presented work relating the development of a compact robotic device able to reach faraway objects that, in our opinion, can have applications in space or planetary missions. We extended applicability of the *casting manipulation* technique to fetch moving objects, and showed two control schemes that can be used to plan the steering phase in realtime. Effectiveness of such schemes was validated through experiments. We also introduced the so-called "3-dimensional casting manipulation" by discussing design and time-optimal control of a robotic manipulator able to steer its end-effector's dynamics in 3D-space. Some simulation results were preliminary reported.

Acknowledgment

Authors would like to acknowledge Hitoshi Arisumi for inspiring this research during his post-doctoral stay in Pisa, and Giovanni Tonietti for helpful discussions.

References

[1] O. Khatib, K. Yokoi, K. Chang, D. Ruspini, R. Holmberg, and A. Casal, "Vehicle/arm coordination and multiple mobile manipulator decentralized cooperation," *Proc. IEEE International Conference on Intelligent Robots and Systems*, 1996.

[2] R. Mamen, "Applying space technologies for human benefit: the canadian experience and global trends," *Canadian Space Agency*.

[3] H. Mochiyama, E. Shimemura, and H. Kobayashi, "Shape correspondence between a spatial curve and a manipulator with hyper degrees of freedom," *Proc. IEEE International Conference on Intelligent Robots and Systems*, 1998.

[4] N. T. et al., "Simulated and experimental results of dual resolution sensor based planning for hyper redundant manipulators," *Proc. IEEE International Conference on Intelligent Robots and Systems*, 1993.

[5] H. Arisumi, T. Kotoku, and K. Komoriya, "Swing motion control of casting manipulation," *IEEE Control Systems*, 1999.

[6] H. Arisumi and K. Komoriya, "Posture control of casting manipulation," *Proc. IEEE International Conference on Robotics and Automation*, 1999.

[7] ——, "Study on casting manipulation (midair control of gripper by impulsive force)," *Proc. IEEE International Conference on Intelligent Robots and Systems*, 1999.

[8] ——, "Catching motion of casting manipulator," *Proc. IEEE International Conference on Intelligent Robots and Systems*, 2000.

[9] A. Fagiolini, H. Arisumi, and A. Bicchi, "Visual-based feedback control of casting manipulation," *Proc. IEEE International Conference on Robotics and Automation*, pp. 2203–2208, 2005.

[10] H. Arisumi, T. Kotoku, and K. Komoriya, "A study of casting manipulation (swing motion control and planning of throwing motion," *Proc. IEEE International Conference on Robotics and Automation*, 1997.

[11] ——, "Swing motion control of casting manipulation (experiment of swing motion control)," *Proc. IEEE International Conference on Robotics and Automation*, 1998.

[12] ——, "Study on casting manipulation (experiment of swing control and throwing)," *Proc. IEEE International Conference on Intelligent Robots and Systems*, 1998.

[13] A. D. Luca and G. Oriolo, "Motion planning under gravity for underactuated three-link robots," *Intelligent Robots and Systems*, 2000.

[14] H. Arisumi, K. Yokoi, and K. Komoriya, "Casting manipulation (braking control for catching motion)," *Proc. IEEE International Conference on Robotics and Automation*, 2000.

[15] A. Namiki, T. Komuro, and M. Ishikawa, "High-speed sensory-motor fusion for robotic grasping," *Measurement Science and Technology*, vol. 13, 2002.